Take your Positions and Shine: Effects of Positioning Aggregation-Induced Emission Luminophores within Sequence-Defined Macromolecules

Peter Pasch,[a] Matthias Killa,[b] Hauke Lukas Junghans,[a] Melanie Schmidt,[a] Stephan Schmidt,[a] Jens Voskuhl,*[b] and Laura Hartmann*[a]

In memory of Carsten Schmuck

Abstract: A luminophore with aggregation-induced emission (AIE) is employed for the conjugation onto supramolecular ligands to allow for detection of ligand binding. Supramolecular ligands are based on the combination of sequence-defined oligo(amidoamine) scaffolds and guanidiniocarbonyl-pyrrole (GCP) as binding motif. We hypothesize that AIE properties are strongly affected by positioning of the luminophore within the ligand scaffold. Therefore, we systematically investigate the effects placing the AIE luminophore at different positions within the overall construct, for example, in the main or side chain of the olig(amidoamine). Indeed, we can show that the position within the ligand structure strongly affects AIE, both for the ligand itself as well as when applying the ligand for the detection of different biological and synthetic polyanions.

Introduction

The concept of aggregation-induced emission (AIE) was introduced by Tang in 2001.[1–3] In contrast to the well-known quenching of fluorescence by aggregation of a fluorophore, AIE luminophores do not emit in the dissolved state but only when restricting their intramolecular rotation or vibration (RIR or RIV), for example through aggregation or in the solid state.[4] Today, a wide range of AIE luminophores has been developed and explored in various applications such as in high-performance OLEDs[5,6] or organic lasers.[7,8] Another interesting area of application is the use of AIE luminophores as optical sensor or marker: binding or complex formation of the AIE with the compound that is supposed to be detected leads to RIR and thus to an increase in emission. This can then be detected and correlated to the binding event. Such AIE sensors have been developed towards the recognition of chemicals compounds such as explosives[9] or vapors[10] and bioamines.[11] Furthermore, they can be applied as biosensors for the detection of amino acids and proteins or for monitoring conformational changes of DNA or proteins[4,12] as well as bioimaging.[13] Along those lines, AIEs can also serve as a biomarker for diagnosing diseases as recently demonstrated by Lou and Xia for a real-time quantitative light detection of telomerase in the urine of bladder cancer patients with a cationic AIE tetraphenylethene derivative.[14]

When developing such novel biomarkers or biosensors, the luminophore has to be modified in a way that allows for strong and ideally specific binding to the target molecule. Usually this is achieved either by bioconjugation for example of a peptide or antibody, or by introducing non-natural recognition motifs such as charged groups or supramolecular binding motifs.[15] In comparison to bioconjugation, non-natural recognition motifs potentially can address new or alternative binding sites of the target molecule and avoid the risk of side effects for example through immunological or cytotoxic responses when used in vitro or in vivo.

In 1999 Schmuck and coworkers introduced the guanidiniocarbonyl-pyrrole (GCP) as supramolecular binding motif.[16,17] The GCP is an arginine mimetic and binds oxyanions such as anionic amino acids on protein surfaces via a hydrogen-bond-assisted ion pairing.[18,19] They have also already demonstrated that by combining multiple GCP motifs on a scaffold, higher affinity and selectivity can be achieved.[20] However, one of the major challenges remains in the detection and analysis of binding of such supramolecular ligands on the target. Therefore, in this work, we combine the use of AIEs for detection of

[a] P. Pasch, H. L. Junghans, M. Schmidt, Jun.-Prof. Dr. S. Schmidt, Prof. Dr. L. Hartmann
Department for Organic Chemistry and Macromolecular Chemistry
Heinrich Heine University Duesseldorf
Universitätsstraße 1, Düsseldorf 40225 (Germany)
E-mail: laura.hartmann@hhu.de

[b] M. Killa, Jun.-Prof. Dr. J. Voskuhl
Faculty of chemistry (Organic chemistry) and CENIDE
University of Duisburg Essen
Universitätsstrasse 7, 45141 Essen (Germany)
E-mail: jens.voskuhl@uni-due.de

Supporting information for this article is available on the WWW under https://doi.org/10.1002/chem.202101086

binding with the GCP functionalized scaffolds as supramolecular binding unit.

For a luminophore construct to be used as an AIE-based sensor, it should be flexible or completely dissolved without the presence of the target molecule, thereby giving no AIE response. Only upon binding to the target or aggregation, the motion is restricted giving rise to AIE and thereby read-out of the binding event. Therefore, we chose flexible, sequence-defined macromolecules[21] as scaffolds, specifically oligo (amidoamines) accessible via so-called solid-phase polymer synthesis[22–25] and allowing for site-specific introduction of both AIE and GCP motifs. We have recently demonstrated that such sequence-defined GCP-functionalized oligo(amidoamines) can act as inhibitors of protein-protein interactions.[26] Since the AIE properties and specifically its emission upon aggregation can be expected to be strongly affected by attachment to the scaffold, in this study we systematically investigate the effects of the position of the AIE within the overall construct. Based on our findings, in the future, GCP oligomers could be designed allowing for both, inhibition of protein-protein interactions and direct read-out of ligand-protein binding via the AIE luminophore.

Results and Discussion

Overall five AIE modified GCP functionalized oligomers (**O1**-**O5**) were synthesized. The AIE luminophore, based on aromatic thioethers described by Voskuhl et al.,[27,28] varies in its position from the direct vicinity of the binding motif to the middle of the side chain or main chain to the position as end group of the oligomer (Scheme 1). All oligomers were synthesized using previously established solid phase polymer synthesis protocols, combining tailor-made building blocks such as EDS (4-((2-(2-(2-aminoethoxy)ethoxy)ethyl)-amino)-4-oxobutanoic),[25] commercially available amino acids such as N_α-Fmoc-N_β-Boc-L-2,3-diaminopropionic acid (DAP), carboxy-functionalized GCP building block and carboxylated aromatic thioether (CATE) as AIE.[29]

In short, the synthesis started from an amine functionalized resin and employed the stepwise addition of building blocks, which carried a free carboxy-group for attachment onto the resin and a protected amine group. Upon successful coupling of the first building block, the protecting group, here fluorenylmethoxycarbonyl (Fmoc), was released and the next building block can be coupled. For the introduction of side chains and attaching GCP and/or AIE motifs, *tert*-butyloxycarbonyl (Boc-) protected DAP was used. Boc can be selectively cleaved on solid phase by using 4 M HCl in dioxane solution,

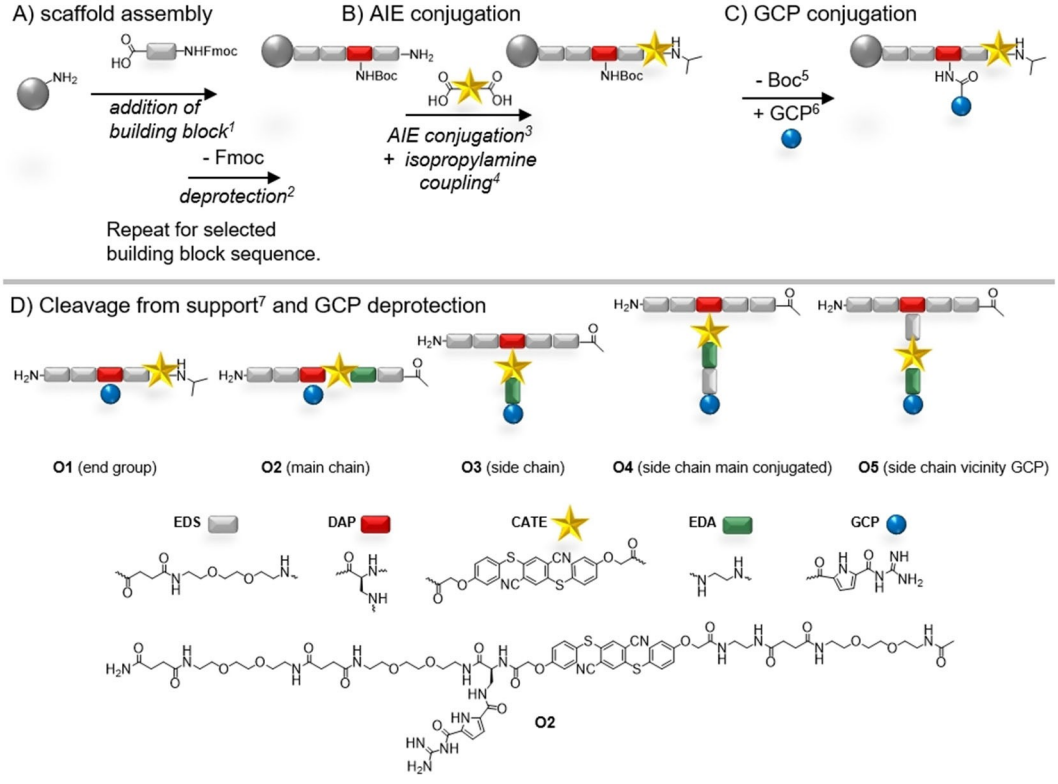

Scheme 1. Synthesis of AIE- and GCP-functionalized oligomers 1–5 using solid phase polymer synthesis. Reaction conditions: 1) 5 equiv. building block, 5 equiv. PyBOP, 10 equiv. DIPEA in DMF, 90 min/2) 25 v% piperidine in DMF, 20 min, 3) 10 equiv. CATE, 10 equiv. PyBOP, 20 equiv. DIPEA in DMF, 48 h, 4) 5 equiv. Isopropylamine, 5 equiv. PyBOP, 10 equiv. DIPEA in DMF, 90 min/ Ac2O, 20 min (acetylation of N-terminus), 5) 4 M HCl in dioxane, 20 min (on-resin cleavage of Boc), 6) 5 equiv. (Boc)GCP-COOH, 5 equiv. PyBOP, 10 equiv. DIPEA in DMF, 90 min (double coupling), 7) TentaGel® S RAM: 5% triisopropylsilane, 95% TFA, 90 min.

thus allowing for coupling of building blocks and constructing the side chain at this position.

Since CATE, synthesized in a three step reaction sequence,[29] carries two carboxylic groups, it can either be placed within the scaffold, as a side chain, or end group. When placed within the scaffold, the remaining carboxylic groups after coupling was activated on solid support and coupled with ethylene diamine to give an amine group for attachment of the next building block. All oligomers were isolated after cleavage from the resin and purification by preparative HPLC as their formate salts with relative purities $>95\,\%$ (as determined by RP-HPLC) and further characterized by ^{1}H NMR and UHR-MS (see Supporting Information).

With these molecules in hand, we investigated their fluorescence properties in solid state in order to know the initial fluorescence of the compounds as a powder. All compounds showed emission maxima in the range of 455 nm ± 5 nm, meaning for our five compounds the AIE position has no influence on the emission behavior in the solid state (see Supporting Information, Figure S20).

We then looked at the AIE behavior in solution. For this purpose, we examine their fluorescence properties first without the presence of a potential binder but already looking at conditions typical for later biological testing (10 mM HEPES buffer at pH 7.4 and 6.5). The selected two pH values allow us to study the start fluorescence in uncharged and charged state of the binding motif, GCP ($pK_a = 6.6$). At a pH value of 7.4 the GCP is uncharged and at 6.5 it is mostly cationic. In general, for oligomers **O1**-**O5**, the AIE luminophore absorbed at 380 nm and emitted in the range of 425–575 nm (see concentration series in water Supporting Information). First, we look at the fluorescence of the oligomers at pH 7.4 at a concentration of 9.71 to 9.77 μM (Figure 1A). We observed weak fluorescence signals of the oligomers with an emission maximum at 450 nm. Compound **O4** had the lowest starting fluorescence suggesting that the AIE luminophore is not or only to a very minor degree restricted in its motion. In general, all oligomers where the luminophore was incorporated in the side chain (**O3**-**O5**) showed a lower starting fluorescence intensity than the derivatives where the luminophore was conjugated in the main chain (**O1**, **O2**). In comparison, **O1**, where the luminophore was incorporated at the end of the main chain, showed the highest fluorescence intensity, indicating AIE-effects. We attribute this to differences in the inter- and intramolecular interactions of the different structural units such as H-bonds of the amide groups, π-π stacking as well as cationic-aromatic interactions of the luminophore and the GCP motif based on their position within the oligomer. To evaluate this further, we reduced the pH value to 6.5. Figure 1B shows the emission maxima of **O1**-**5** at pH 7.4 compared to 6.5 at identical fluorescence settings. In general, the emission intensity of all compounds at pH 6.5 increased. We attribute this to additional cationic-aromatic interactions caused by the cationic charge of the GCP[30] that lead to more pronounced inter- and intramolecular interactions. The fluorescence at lower pH is thus a first insight into a potential bound or aggregated state of the AIE oligomers and thus their ability to change fluorescence upon interaction with

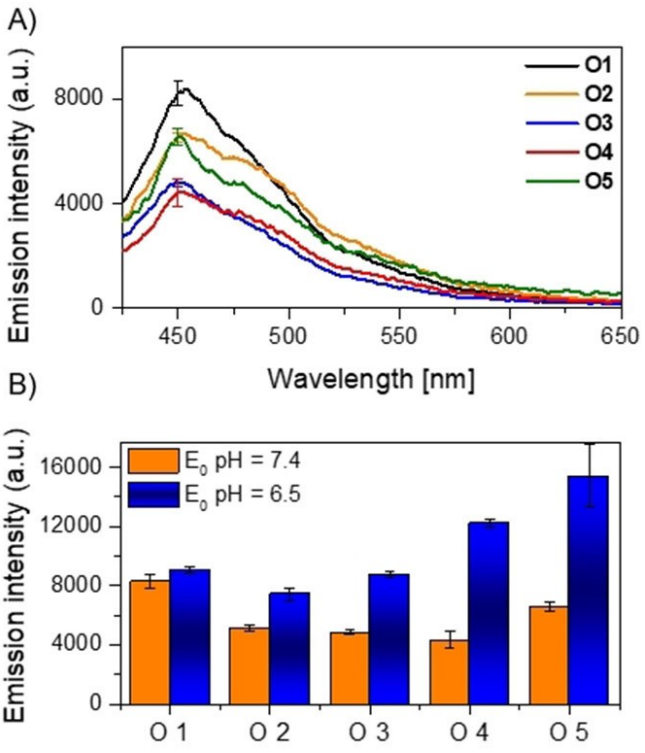

Figure 1. A) Starting fluorescence spectra of **O1**-**5** (9.74 μM; 9.71 μM; 9.75 μM; 9.77 μM; 9.77 μM) in 10 mM HEPES buffer at pH = 7.4, (Triplicates, $\lambda_{ex} = 380$ nm). B) Starting fluorescence maxima at 450 nm of **O1**-**5** in 10 mM HEPES buffer at pH = 7.4 and 6.5 (Triplicates, $\lambda_{ex} = 380$ nm).

a target structure. The increase in fluorescence was more pronounced for oligomers where the luminophore was side chain conjugated (**O3**-**O5**). This indicates that side chain conjugated oligomers could be more beneficial to allow for AIE behavior in solution as the luminophore remains less restricted by the scaffold itself when positioned in the side chain. Comparing compounds **O4** and **O5** carrying an additional hydrophilic building block in the side chain, this effect was more pronounced than for **O3**, supporting the idea that more flexibility in the non-bound state of the AIE-oligomer gives more pronounced AIE effects upon binding and/or aggregation.

In order to further evaluate the AIE behavior when bound to a potential target structure and to explore the potential use of the AIE oligomers as biosensors, we screened for potential binding partners. In our ligand design we applied GCP as binding unit. GCP is known to bind to oxyanions of various types, for example carboxylates[16] or phosphates,[31] therefore we chose a range of anionic molecules and materials: bovine serum albumin (BSA), concanavalin A (Con A), esterase and 14-3-3ζ were selected as proteins with an isoelectric point at or even below pH 5.[32] Additionally trypsin with an isoelectric point of almost 11 was selected for comparison.[33] In addition to the proteins, heparin and RNA as natural and poly(acrylic acid) (PAA) as non-natural polyanions were tested. Phosphate-buffered saline (PBS) was used as a small molecule anion along with sodium dodecyl sulfate (SDS) above its critical micelle concentration to give anionic micelles. As larger materials with

sizes on the order of 500 nm, poly(*N*-isopropylacrylamide) microgels (MGs) containing 2% or 5% methacrylic acid as anionic comonomer (MG 2% and MG 5%) were included in this study.[34] Overall this offers a range of anionic materials of different size as well as charge density. AIE GCP oligomers were titrated against the different anionic compounds and emission was measured at 450 nm. Figure 2 depicts the differences observed for emission of the pure oligomers (E_0) divided by the emission detected for the mixture with the according anionic compound (E). Values for $E/E_0 = 1$ showed no AIE effect, values >1 showed an increased emission upon mixing with the anionic compound and thus an AIE effect. Values that go below 1 would indicate fluorescence quenching. Surprisingly, we observed only very little AIE response, if at all, for oligomers **O1**-**O3** and **O5**. Only **O4** showed a clear increase in emission upon mixing with anionic MGs and PAA, less pronounced in mixtures with BSA, esterase, heparin, PBS, 14-3-3ζ and RNA. It is noticeable that **O4** could achieve an AIE effect with anionic phosphates presented on RNA or in PBS as well as anionic amino acids on protein surfaces though these effects are not as pronounced. This can probably be attributed to the higher density of anionic groups within the polyanions in comparison to the proteins, as we also observed a stronger AIE effect for the MGs with a higher density of anionic groups, i.e. when comparing MG 5% vs. MG 2%. Overall, the AIE effect observed for our oligomers is not extremely high yet significant and well in the range of other ligands described in literature that have successfully used emission changes to detect ligand binding.[35,36]

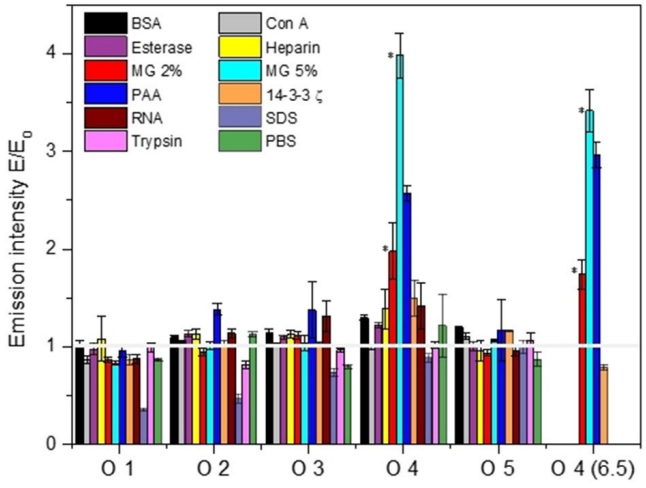

Figure 2. Change in fluorescence emission of **O1**-**5** (9.74 μM; 9,71 μM; 9.75 μM; 9.77 μM; 9.77 μM) in the presence of different anionic molecules, aggregates and materials measured in 10 mM HEPES buffer at pH = 7.4, (Triplicates, $\lambda_{ex} = 380$ nm, $\lambda_{em} = 450$ nm, E = Final Emission, E_0 = Start; BSA, Con A, Heparin, PAA, PBS, Trypsin and 14-3-3 ζ 10 μM; Esterase and Micro gel (NIPAM-*co*-MAA Copolymer) 2 and 5%, RNA 100 μg/ml and SDS 10 mM) and **O4** (6.5) (10 mM HEPES buffer at pH = 6.5) PAA, Micro gel (NIPAM-co-MAA Copolymer) 2 and 5%. Samples that showed turbidity are marked with *.

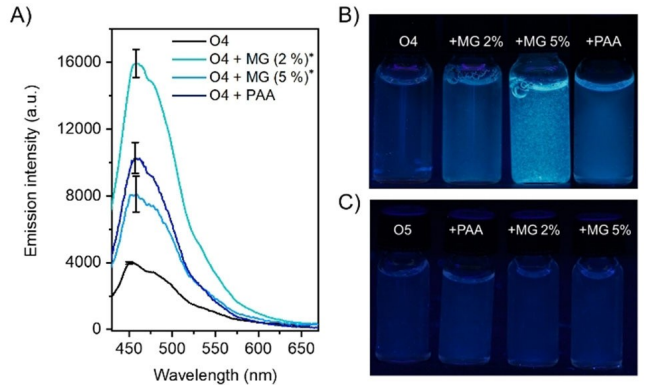

Figure 3. A) Fluorescence spectra of **O4** (9.77 μM) pure (black) and in the presence of MG 2% 100 μg/ml, MG 5% 100 μg/ml and PAA 10 μM (triplicates, $\lambda_{ex} = 380$ n, $\lambda_{em} = 450$ nm). Samples that showed turbidity are marked with *. Comparison of fluorescence emission of B) **O4** and C) **O5** (both 9.77 μM) with and without anionic binders. Reflection effects on the glass surface were removed using GIMP 2.10 software.

Figure 3 highlights the differences between **O4** (Figure 3B), and **O5** (Figure 3C) as exemplary non-AIE oligomer when binding to MGs and PAA. Also optically, the AIE effects were clearly visible for **O4** in contrast to **O5** with no increase in emission upon mixing with any of the anionic compounds. When looking at the emission maxima (Figure 3A), of **O4** when binding to MGs or PAA, we saw a slight shift to higher wavelengths from 450 nm for pure **O4** up to 462 nm by addition of MG 5%. This red-shift in the emission spectra could be attributed to the close proximity of the AIE fluorophore to the polar carboxylates when the oligomer binds to the anionic material. For anionic microgels we even observed turbidity which indicates a screening of the stabilizing charges and aggregation of MGs which would in turn further promote AIE effects.

Next, we looked at the resulting changes for the AIE effect of **O4** with selected materials at pH 6.5 instead of pH 7.4. We selected MGs, PAA and 14-3-3ζ, as they already showed AIE effects at pH 7.4. For 14-3-3ζ, **O4** showed no more AIE effect at pH 6.5. We attribute this to the increased number of cationic amino acids on the protein surface, which interfered with the binding of cationic GCP of **O4** to 14-3-3ζ.

For MGs and of PAA, on the other hand, we still observed a clear AIE effect also at pH 6.5. Again, the most pronounced AIE effects in this series were achieved with MG 5%. Interestingly, as the PAA fluorescence intensity is higher at pH 6.5, this system seems to profit more from the increased cationic charge of the GCP units. This could potentially be a concentration dependent effect, where the ratio of anionic groups to GCP motifs could also affect the complex formation and thus AIE read out.

To further investigate the concentration dependence of the AIE effect, we looked at two titration series of PAA to the oligomer **O4**. Figure 4A shows the AIE effects of the titration of PAA. We started at a ratio of 1 μM PAA to 9.77 μM oligomer, which corresponds to about 10 molecules of **O4** per PAA chain with an average of 6250 acrylic acid side chains. Next, we further increased the amount of PAA thereby diluting the ratio of oligomer per PAA. Within the error margins of these experiments, we saw a slight decrease in AIE with increasing concentration of PAA but the AIE effect remained indicating

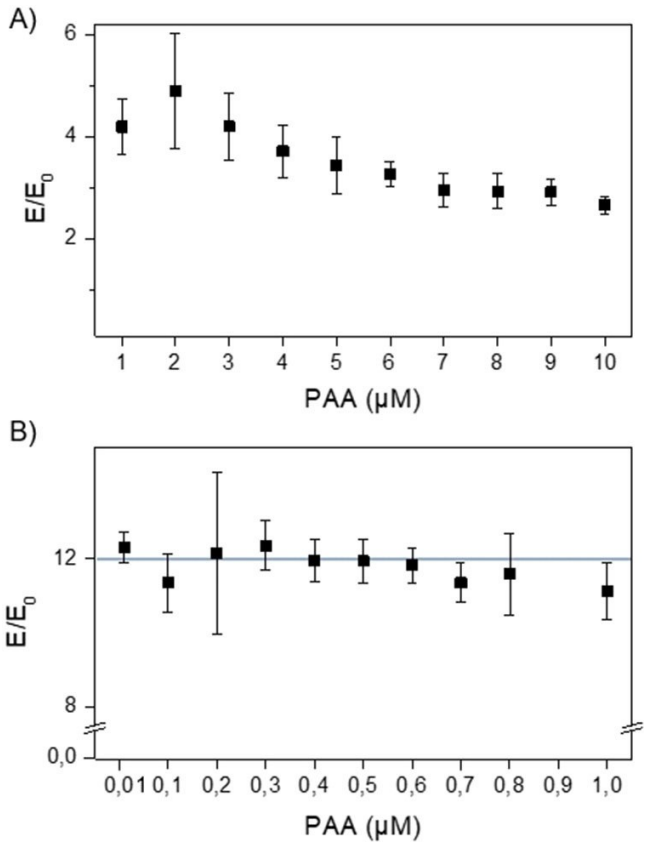

Figure 4. Change in fluorescence emission of **O4** (9.77 μM) in the presence of PAA A) 1–10 μM and B) 0.01–1 μM; both assays in 10 mM HEPES buffer at pH = 7.4, (triplicates, λ_{ex} = 380 nm, λ_{em} = 450 nm, E = Final Emission, E_0 = Start). In concentration series B, turbidity was observed for all samples.

that interaction of the oligomer and the polyanion lead to some change in vibrational and/or rotational freedom of the fluorophore. When performing the titration starting from a higher ratio of oligomer per PAA chain, 0.01 to 1 μM of PAA (Figure 4B), we observed a stronger AIE effect that was accompanied by turbidity in all samples. Higher concentrations of **O4** more effectively shield the anionic charge of the PAA chains, leading to destabilization and aggregation. As could be expected, for these samples an overall higher AIE effect was observed. Overall, these experiments demonstrate that **O4** showed AIE behavior over a wide range of concentrations. For a potential application in biological settings this could indeed be an important feature as concentrations of a target protein for example inside a cell or cellular compartment might not be known.

The oligomer fluorescence properties without the presence of anionic binder, indicate that intra- and intermolecular interactions of the oligomers in solution affect their AIE properties. In order to investigate intermolecular interactions in more detail, we analyzed the oligomer aggregation behavior in water via atomic force microscopy (AFM) and scanning electron microscopy (SEM).

All samples were prepared from 100 μM aqueous solution and dried by spincoating prior to sample analysis. Figure 5 shows representative AFM data for all oligomers (for detailed zoomed in data see Supporting Information). Similar structures for the different samples were also observed by SEM (see Supporting Information). Indeed, we saw clear differences between the different oligomers. Particularly oligomer **O2** formed network like structures whereas **O3**-**O5** showed shorter linear structures and **O1** showed spherical aggregates. We hypothesize that when positioning the AIE at the end of the main chain end, as in **O1**, we induce an amphiphilic character of the overall oligomer which in turn could lead to the formation of spherical aggregates, similar to micelles. When moving the AIE more towards the middle of the scaffold, amphiphilicity seems to be reduced and we observed network formation of **O2**. Similar effects have been already described for other AIE luminophore systems, for example Gonzalez-Rodriguez et al. as well as B. Z. Tang showed the occurrence of network formation induced by π-π interactions of the AIE luminophores, which are supported by additional hydrogen bonds to large defined superstructures.[37,38] When moving the AIE into the side chain of the oligomer, we still observed aggregates that were smaller and linear rather than larger networks. The stacking of oligomers is likely less ordered when going from linear to branched oligomers as is the case when moving from **O2** to **O3**-**O5**. This is in line with similar observations on linear and branched polymers, where an increase in branching reduces intermolecular interactions and thereby increases the free volume and flexibility of the chains.[39] It is thus not surprising that a branched oligomer, **O4**, was the one oligomer that showed AIE behavior.

When comparing the three branched oligomers of this series, **O3**-**O5**, the main difference between **O3**/**O5** (showing no AIE) and **O4** (showing AIE) is the relative positioning of the AIE luminophore and the binding GCP unit. In **O3** and **O5**, luminophore and GCP were placed next to each other, while in **O4** we added a spacer building block introducing an additional diethyleneglycol linker in between. We originally rationalized

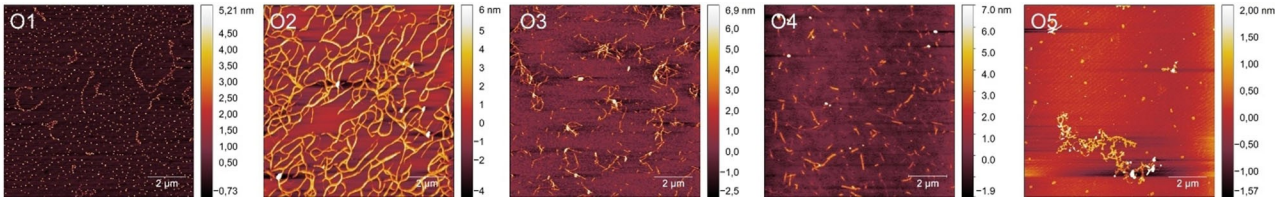

Figure 5. Atomic force microscope images of **O1**-**5** (100 μM in Millipore water). Further AFM, SEM images and their analysis see the Supporting Information.

that a closer proximity of luminophore and binding unit should be beneficial for the AIE effect, in order to enable a more pronounced change in rotational and vibrational freedom upon binding of the GCP unit. However, unexpectedly, only the introduction of an additional linker between luminophore and binding unit leads to an AIE active oligomer. Future studies will explore this effect further by synthesizing oligomers with additional linker units of different length and flexibility as well as for oligomers presenting multiple GCP motifs, thereby looking more closely at the interplay of inter- and intramolecular interactions.

Conclusion

In summary, we realized the sequence-defined positioning of an AIE luminophore within oligomers presenting the supramolecular binding motif GCP. Surprisingly, we found that only one of the oligomeric structures of this study showed an AIE effect in solution when interacting with anionic structures. The fluorescence results demonstrate that indeed the positioning of AIE luminophore and binding motif (here GCP) within an oligomeric ligand affect the ability of the luminophore to show AIE behavior. None of the oligomers that has the AIE luminophore in the main chain and directly attached the GCP motif to the main chain show AIE behavior in solution. However, also for the side chain constructs, a fine differentiation was observed in terms of the relative positioning of AIE and GCP. It seems that directly linking AIE and GCP motifs through the ethylene diamine linker does not allow for AIE behavior, while introducing an additional EDS building block lead to **O4** and clear AIE properties. Based on our findings we can now further develop sequence-defined oligomers carrying both, supramolecular binding motifs and AIE luminophores, and explore their potential as biosensors.

Acknowledgements

The authors acknowledge funding from the DFG through the collaborative research center 1093 (projects A10, A11 and A1). We thank Christian Ottmann for providing 14-3-3ζ and Tobias Wilcke and Henning Berens for taking the photos for Figure 3. We thank Steffen Riebe for helping with the initial synthesis of the AIE luminophore. We thank Tobias Bochmann for scanning electron microscopy. Open access funding enabled and organized by Projekt DEAL.

Conflict of Interest

The authors declare no conflict of interest.

Keywords: aggregation induced emission · biosensors · sequence-defined oligomers · solid phase polymer · supramolecular synthesis

[1] H. Fang, S. Xu, Bin Liu, *Adv. Mater.* **2018**, *30*, 1801350.
[2] Y. Hong, *Methods Appl. Fluoresc.* **2016**, *4*, 022003.
[3] J. Luo, Z. Xie, J. W. Y. Lam, L. Cheng, H. Chen, C. Qiu, H. S. Kwok, X. Zhan, Y. Liu, D. Zhuc, B. Z. Tang, *Chem. Commun.* **2001**, *18*, 1740–1741.
[4] J. Liang, B. Z. Tang, B. Liu, *Chem. Soc. Rev.* **2015**, *44*, 2798–2811.
[5] Z. Zhao, J. W. Y. Lam, B. Z. Tang, *J. Mater. Chem.* **2012**, *22*, 23726–23740.
[6] Z. Zhao, B. He, B. Z. Tang, *Chem. Sci.* **2015**, *6*, 5347–5365.
[7] X. Gu, J. Yao, G. Zhang, Y. Yan, C. Zhang, Q. Peng, Q. Liao, Y. Wu, Z. Xu, Y. Zhao, H. Fu, D. Zhang, *Adv. Funct. Mater.* **2012**, *22*, 4862–4872.
[8] X. Gu, J. Yao, G. Zhang, C. Zhang, Y. Yan, Y. Zhao, D. Zhang, *Chem. Asian J.* **2013**, *8*, 2362–2369.
[9] H. Zhou, M. H. Chua, B. Z. Tang, J. Xu, *Polym. Chem.* **2019**, *10*, 3822–3840.
[10] M. Gao, S. Li, Y. Lin, Y. Geng, X. Ling, L. Wang, A. Qin, B. Z. Tang, *ACS Sens.* **2016**, *1*, 179–184.
[11] M. Hayduk, S. Riebe, K. Rudolph, S. Schwarze, F. van der Vight, C. G. Daniliuc, G. Jansen, J. Voskuhl, *Isr. J. Chem.* **2018**, *58*, 927–931.
[12] R. T. K. Kwok, C. W. T. Leung, J. W. Y. Lam, B. Z. Tang, *Chem. Soc. Rev.* **2015**, *44*, 4228–4238.
[13] S. Riebe, C. Vallet, F. van der Vight, D. Gonzalez-Abradelo, C. Wölper, C. A. Strassert, G. Jansen, S. Knauer, J. Voskuhl, *Chem. Eur. J.* **2017**, *23*, 13660–13668.
[14] I. M. Khan, S. Niazi, M. K. Iqbal Khan, I. Pasha, A. Mohsin, J. Haider, M. W. Iqbal, A. Rehman, L. Yue, Z. Wang, *TrAC Trends Anal. Chem.* **2019**, *119*, 115637.
[15] a) L. A. Logsdon, C. L. Schardon, V. Ramalingam, S. K. Kwee, A. R. Urbach, *J. Am. Chem.* **2011**, *133*, 17087–17092; b) F. Trusch, K. Kowski, K. Bravo-Rodriguez, C. Beuck, A. Sowislok, B. Wettig, A. Matena, E. Sanchez-Garcia, H. Meyer, T. Schrader, P. Bayer, *Chem. Commun.* **2016**, *52*, 14141–14144; c) J. Matic, F. Supljika, N. Tir, P. Piotrowski, C. Schmuck, M. Abramic, I. Piantanida, S. Tomic, *RSC Adv.* **2016**, *6*, 83044.
[16] C. Schmuck, *Chem. Eur. J.* **2000**, *6*, 709–718.
[17] C. Schmuck, J. Lex, *Org. Lett.* **1999**, *1*, 1779–1781.
[18] C. Schmuck, *Coord. Chem. Rev.* **2006**, *250*, 3053–3067.
[19] J. Matić, F. Šupljika, T. Tandarić, M. Dukši, P. Piotrowski, R. Vianello, A. Brozovic, I. Piantanida, C. Schmuck, M. R. Stojković *Int. J. Biol. Macromol.* **2019**, *134*, 422–434.
[20] M. Giese, J. Niemeyer, J. Voskuhl, *ChemPlusChem* **2020**, *85*, 985.
[21] a) M. A. R. Meier, C. Barner-Kowollik, *Adv. Mater.* **2019**, *31*, 1806027; b) W. Konrad, F. R. Bloesser, K. S. Wetzel, A. C. Boukis, M. A. R. Meier, C. Barner-Kowollik, *Chem. Eur. J.* **2018**, *24*, 3413.
[22] D. Ponader, F. Wojcik, F. Beceren-Braun, J. Dernedde, L. Hartmann, *Biomacromolecules* **2012**, *13*, 1845–1852.
[23] C. Gerke, F. Jacobi, L. E. Goodwin, F. Pieper, S. Schmidt, L. Hartmann, *Macromolecules* **2018**, *51*, 5608–5619.
[24] S. Boden, F. Reise, J. Kania, T. K. Lindhorst, L. Hartmann, *Macromol. Biosci.* **2019**, *19*, 1800425.
[25] a) C. Gerke, M. F. Ebbesen, D. Jansen, S. Boden, T. Freichel, L. Hartmann, *Biomacromolecules* **2017**, *18*, 787–796; b) M. F. Ebbesen, C. Gerke, P. Hartwig, L. Hartmann, *Polym. Chem.* **2016**, *7*, 7086–7093.
[26] P. Pasch, A. Höing, S. Ueclue, M. Killa, J. Voskuhl, S. K. Knauer, L. Hartmann, *Chem. Commun.* **2021**, *57*, 3091–3094.
[27] a) J. Stelzer, C. Vallet, A. Sowa, D. Gonzalez-Abradelo, S. Riebe, C. G. Daniliuc, M. Ehlers, C. A. Strassert, S. K. Knauer, J. Voskuhl, *ChemistrySelect* **2018**, *3*, 985–991; b) P. Ahlers, C. Götz, S. Riebe, M. Zirbes, M. Jochem, D. Spitzer, J. Voskuhl, T. Basché, P. Besenius, *Polym. Chem.* **2019**, *10*, 3163–3169.
[28] a) S. Riebe, C. Wölper, J. Balszuweit, M. Hayduk, M. E. Gutierrez Suburu, C. A. Strassert, N. L. Doltsinis, J. Voskuhl, *ChemPhotoChem* **2020**, *4*, 383–384; b) H. Frisch, D. Spitzer, M. Haase, T. Basché, J. Voskuhl, P. Besenius, *Org. Biomol. Chem.* **2016**, *14*, 5574–5579.
[29] a) C. Schmuck, V. Bickert, M. Merschky, L. Geiger, D. Rupprecht, J. Dudaczek, P. Wich, T. Rehm, U. Machon, *Eur. J. Org. Chem.* **2008**, *2*, 324–329; b) M. Externbrink, S. Riebe, C. Schmuck, J. Voskuhl, *Soft Matter* **2018**, *14*, 6166–6170.
[30] J. Hatai, C. Schmuck, *Acc. Chem. Res.* **2019**, *52*, 1709–1720.
[31] S. Junghänel, S. Karczewski, S. Bäcker, S. K. Knauer, C. Schmuck, *ChemBioChem* **2017**, *18*, 2268–2279.
[32] a) W. S. Ang, M. Elimelech, *J. Membr. Sci.* **2007**, *296*, 83–92; b) G. Entlicher, J. V. Koštíř, J. Kocourek, *Biochim. Biophys. Acta* **1971**, *236*, 795–797; c) D. Wynne, Y. Shalitin, *Arch. Biochem.* **1973**, *154*, 199–203.
[33] M. Bier, F. F. Nord, *Arch. Biochem.* **1951**, *33*, 320–332.
[34] a) S. Schmidt, T. Hellweg, R. von Klitzing, *Langmuir* **2008**, *24*, 12595–12602; b) S. Schmidt, H. Motschmann, T. Hellweg, R. von Klitzing, *Polymer* **2008**, *49*, 749–756; c) T. Hoare, R. Pelton, *Langmuir* **2004**, *20*,

2123–2133; d) A. Strzelczyk, T. J. Paul, S. Schmidt, *Macromol. Biosci.* **2020**, *20*, 2000186.
[35] D. Maity, A. Gigante, P. A. Sánchez-Murcia, E. Sijbesma, M. Li, D. Bier, S. Mosel, S. Knauer, C. Ottmann, C. Schmuck, *Org. Biomol. Chem.* **2019**, *17*, 4359–4363.
[36] Y. Liu, C. Deng, L. Tang, A. Qin, R. Hu, J. Z. Sun, B. Z. Tang, *J. Am. Chem. Soc.* **2011**, *133*, 660–663.
[37] D. Gonzalez-Rodriguez, A. P. H. J. Schenning, *Chem. Mater.* **2011**, *23*, 310–325.
[38] J. Li, J. Wang, H. Li, N. Song, D. Wang, B. Z. Tang, *Chem. Soc. Rev.* **2020**, *49*, 1144–1172.
[39] a) L. J. Markoski, J. S. Moore, I. Sendijarevic, A. J. McHugh, *Macromolecules* **2001**, *34*, 2695; b) J. Peter, A. Khalyavina, J. Kriz, M. Bleha, *Eur. Polym. J.* **2009**, *45*, 1716.

Manuscript received: March 25, 2021
Accepted manuscript online: April 20, 2021
Version of record online: May 28, 2021

